Substrate-induced structural modulation of a CoO(111) bilayer on Ir(100)

Christina Ebensperger, Matthias Gubo, Wolfgang Meyer, Lutz Hammer, and Klaus Heinz
Lehrstuhl für Festkörperphysik, Universität Erlangen–Nürnberg, Staudtstr. 7, D-91058 Erlangen, Germany
(Received 14 July 2009; revised manuscript received 4 May 2010; published 3 June 2010)

We report on an unusual structural modulation of a single CoO(111) bilayer grown on Ir(100)-(1×1) by oxidation of slightly less than one monolayer of Co deposited on the substrate. Quantitative low-energy electron diffraction and scanning tunneling microscopy in combination with standard x-ray photoelectron spectroscopy and thermal-desorption spectroscopy reveal a cobalt layer next to the substrate covered by an oxygen layer. Both layers' hexagonal atomic arrangements are, however, strongly distorted by the quadratic substrate and form a $c(10\times2)$ superstructure on that. The Co layer's buckling amplitudes and atomic bond lengths to Ir atoms are consistent with the hard-sphere radius of metallic Co. The oxide's binding to the substrate appears to be further characterized by two types of oxygen ions. One of them is close to the expected rocksalt-type stacking with respect to the cobalt layer while the other type resides nearly on top of Ir atoms. Its hard-sphere radius is only 0.77 Å (in contrast to 1.25 Å in the CoO bulk) and it is by about 1 Å closer to the substrate than the other type. Being so almost coplanar with the Co layer, it locally forms a hexagonal boron-nitride-type oxide. The oxygen bond to Ir can be interpreted as local pinning of the oxide to the substrate so modulating the entire oxide bilayer.

DOI: 10.1103/PhysRevB.81.235405 PACS number(s): 68.47.Gh, 68.35.Ct, 68.55.at, 61.05.jh

I. INTRODUCTION

Recently, nanosized transition-metal oxides have attracted considerable attention in basic and applied research due to their unusual magnetic properties. Among those cobalt oxide of 1:1 stoichiometry (CoO) has gained special interest. It is antiferromagnetic in its native rocksalt structure and has, for example, been used to enclose nanosized cobalt clusters to beat the superparamagnetic limit[1] by the magnetic exchange coupling with the ferromagnetic cobalt. On this background and as the structures of nanosized solids frequently differ from their bulk structures, we have studied ultrathin cobalt-oxide films in the recent past whereby the Ir(100)-(1×1) surface has been used as support.[2] In fact, we have found that the surfaces of CoO films grown in (111) orientation deviate substantially from the rocksalt structure[3,4] [the large lattice misfit between CoO and Ir of about 10% prohibits pseudomorphic growth in (100) orientation].

Of course, such drastic deviations from the bulk structure occur not only at the oxide's surface but may also be induced at its interface to the substrate and this may considerably influence the further film growth. Access to the substrate's influence is possible for ultrathin films as they contain only a few oxide layers so that the substrate is close to the surface. Also, the oxide growth may then be pseudomorphic with a possibly substantial deviation from the oxide's bulk lattice parameter which may severely affect the magnetic properties of the film due to the strong correlation between magnetism and crystallography.[5] Moreover, the film might not only correspond to a strained bulklike phase but may form a completely different two-dimensional structure as outlined in Ref. 6 (and references therein) and as we have very recently shown for a (3×3)-periodic film with Co_8O_5 stoichiometry on Ir(100)-(1×1).[7] We have also reported for this phase that it transforms into a $c(10\times2)$ superstructure by exposure to oxygen, a transition which can be reversed by annealing of the sample accompanied by oxygen loss.[7]

The present paper deals with this $c(10\times2)$ phase which, as has been proposed in earlier work of our group,[7,8] consists of a single CoO(111)-type oxide bilayer and so represents the thinnest possible film of this type. We aim for its crystallographic structure which has been lacking up to now and might be of importance for the understanding of the oxide-substrate interface of already investigated thicker oxide films. To achieve this structure, we apply quantitative low-energy electron diffraction (LEED). As input for the structural analysis, we use atomically resolved images obtained by scanning tunneling microscopy (STM) which are similar to those published already earlier.[8] The cleanness and elemental composition of the oxide film were probed by means of thermal-desorption spectroscopy (TDS) and standard x-ray photoemission spectroscopy (XPS) with calibration achieved by comparison to the known stoichiometry of the above mentioned (3×3)-periodic film.[7]

Next we describe the preparation of the film and substrate, the experimental methods applied and details of the LEED calculations. The preinformation extracted from the experiments is described in the Sec. III, in particular, the cobalt and oxygen content of the film and the crude structural model retrieved. The latter is the starting point of the quantitative LEED analysis which is presented subsequently. The results are discussed in the last but one paragraph followed by the conclusion.

II. EXPERIMENTAL AND COMPUTATIONAL DETAILS

The unreconstructed (100) surface of iridium, Ir(100)-(1×1), is a metastable phase which can be prepared by oxygen-induced lifting of the stable and quasihexagonally reconstructed phase followed by the reduction in oxygen via hydrogen exposure.[9–11] LEED and STM investigations using the (1×1) substrate were carried out in a two-stage ultrahigh-vacuum apparatus. One vessel hosted a homemade LEED optics as well as standard tools for surface analyses

using XPS and TDS (for special features of the latter see Ref. 2). The other vessel contained a commercial beetle-type STM with easy transfer between the two stages.[8] The preparation of the oxide film, which has been slightly improved since our earlier investigation,[8] was by deposition of about 9/10 of a monolayer (ML) of cobalt (with respect to the areal density of substrate atoms, 1.36×10^{15} cm^{-2}), and corresponding to the atomic density of Co in a (111) layer of Co in CoO(111). The deposition rate was about 1 ML/min and the sample was held at 50 °C. The cobalt film was oxidized by exposure to oxygen for about 2 min at a local pressure of 5×10^{-8} mbar with the sample heated to 250 °C. This was followed by a flash to 400 °C upon which a well-ordered $c(10\times2)$ superstructure developed.

STM images were taken at room temperature whereby atomic resolution could be achieved for tip voltages in the millivolt range.[8] Processing of STM data was performed using the program WSXM described in Ref. 12. For the structural analysis, LEED patterns and intensity versus energy spectra were recorded for normal incidence of the primary beam with the sample at liquid-nitrogen temperature and using a computer-controlled video method.[13] Symmetrically equivalent spectra were averaged. The total database of symmetrically inequivalent spectra is as large as 18 000 eV and consists of spectra of 8 integer-order and 42 fractional-order beams in the energy range 40–600 eV.

The crystallographic structure was revealed using the perturbation method TENSORLEED (Refs. 13–15) applying the TENSERLEED code.[16] For the structural search, a frustrated simulated annealing procedure was applied,[17] controlled by the Pendry *R* factor[18] to compare experimental and simulated spectra on a quantitative scale. A maximum of 14 phase shifts calculated as described in Ref. 19 and corrected for thermal diffuse scattering was used. Electron attenuation was simulated as usual by an optical potential which was determined as V_{0i}=5.5 eV. The real part of the inner potential was taken energy dependent according to Ref. 19 in order to account for the energy dependence of the exchange-correlation potential.

III. PREINFORMATION FROM LEED, STM, XPS, AND TDS

Panels (a) and (b) of Fig. 1 display the STM image and LEED pattern of the $c(10\times2)$ superstructure similar to those published earlier.[8] In (a), the noncentered unit cell and in (b), the corresponding reciprocal unit cell is inserted. In order to reduce noise and to get rid of local image properties, the STM signal was averaged over many equivalent unit cells and the resulting average cell was periodically replicated producing the image displayed in panel (c). This procedure produces no features which were not already visible in the original STM image [displayed in panel (a)] but improves recognizability considerably. The profile along the line inserted [panel (d)] exhibits nine protrusions within the unit cell with an apparent buckling amplitude of 0.6 Å (this averaged value is more precise than the value of about 0.5 Å which was reported in earlier work as determined on the basis of a single unit cell[8]). As obvious, four species are

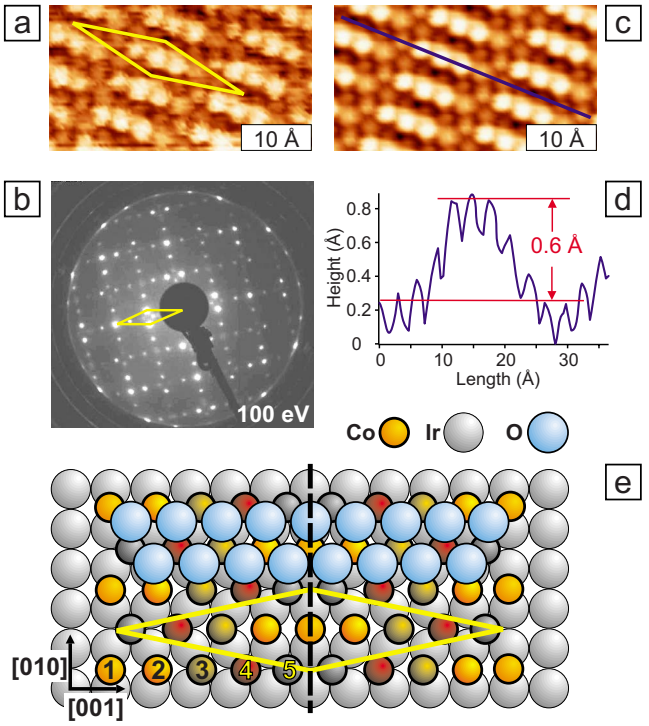

FIG. 1. (Color online) Information from LEED and STM: (a) STM image recorded at 2.2 mV (1.1 nA) and (b) LEED pattern taken at 100 eV electron energy. In (a), the real space, noncentered unit cell is inserted and in (b) its reciprocal equivalent. The STM image in panel (c) results from the periodic repetition of the average unit cell (see text). The height profile along the line inserted is displayed in (d). Panel (e) shows a structural model concluded from the STM image as proposed earlier (Ref. 8). In the lower half, only the cobalt species are displayed, the upper half contains also the oxygen ions arranged in hollow sites formed by Co. The vertical line indicates the mirror-symmetry plane assumed to apply.

closer to the substrate than the remaining five ones. Of course, one can neither directly derive the chemical identity of the imaged species nor, due to electronic effects, the geometrical buckling. Nevertheless, a tentative structural model as displayed in Fig. 1(e) was proposed in our earlier paper.[8] It is based on the assumption that the oxide consists of a slightly distorted CoO(111) bilayer whereby the cobalt layer faces the substrate and is imaged in the STM in spite of the oxygen layer above. Assuming the ionic radius (0.88 Å) of Co in the bulk of CoO, the buckling in the STM image is almost quantitatively reproduced. The distortion of the hexagonal layer is by 4.1% in [010] direction and by 0.3% in [001] direction (we denote such layers as quasihexagonal in the following). The oxygen species were assumed to continue a rocksalt-like stacking, i.e., to sit within hollow sites formed by the Co layer.

The identification of the protrusions in the STM images as Co species corresponds to a cobalt content of 0.90 ML in the film. This is quantitatively in line with work on the epitaxial growth of Co on Ir(100).[8,20] In these investigations, in which the same Co deposition procedure as in the present paper was used, the Co coverage could be determined with high accuracy. As the oxide is produced by oxidation of the already present Co film, the comparison to this former experiments

leads to reliable results. Additionally, we can conclude that there is no relevant diffusion of cobalt into the substrate. Concerning the oxygen content of the oxide, TDS experiments were carried out whereby the oxide decomposes and oxygen desorbs. The TDS peaks were integrated and calibrated by comparison to the equivalent data resulting from spectra of the recently investigated (3×3)-periodic film which is of Co_8O_5 stoichiometry.[7] This yields an oxygen amount of 0.86 ML. Integration of the oxygen peaks applying XPS and again comparison to the Co_8O_5 phase retrieves an oxygen content of 0.90 ML which exactly matches the nominal value of our model. So the O/Co stoichiometry of the oxide is 1:1.

IV. QUANTITATIVE INTENSITY ANALYSIS

For the quantitative LEED intensity analysis of the oxide film (including the first few substrate layers below it), several types of structural models were tested. One of them is that displayed in Fig. 1(e). Additionally, also other physically reasonable models consistent with the STM image were considered, i.e., with quasihexagonal layers and nine species per layer and unit cell. So, a bilayer model with oxygen rather than cobalt facing the substrate was tested. In addition and in spite of the information from TDS and XPS that the film's oxygen content amounts to 0.9 ML, two trilayer models with a O-Co-O layer sequence and either wurtzite-type (as detected for thicker CoO films[3]) or rocksalt-type stacking [as observed for RhO (Ref. 21)] were considered. In these first rough calculations, the positions of the various species were varied only normal to the surface while their lateral positions were fixed according to the quasihexagonal arrangement. All these additional models produced an unsatisfying comparison between model spectra and experimental LEED data corresponding to R factors not lower than 0.5. For the Co-O bilayer (with Co facing the substrate), we also allowed Co rows with their center line above that of substrate atoms and oxygen in top, bridge, and hollow positions of the Co layer. Again these models produced unsatisfying R factors ($R>0.55$). Only the model with Co arranged according to Fig. 1(e) and covered with an oxygen layer with species in cobalt hollow sites produced an R factor of $R\approx0.3$, i.e., low enough to promise a satisfying theory-experiment fit by additional variation in lateral positions of species (though we have no knowledge about their degree of ionicity, we denote these species cobalt or oxygen ions in the following independent of their individual chemical properties or hard-core radii).

Therefore, the further analysis of the LEED intensities concentrated on this model with a Co layer at the interface and the Co ions arranged as rows positioned between [010] or [001] oriented rows of Ir atoms of the (100) surface as shown in Fig. 1(e). As there are two different kinds of hollow sites formed by cobalt and to be occupied by oxygen (equivalent to different stacking of the oxygen on the cobalt layer), two domains have to be considered. The substrate's square symmetry further allows symmetrically equivalent and mutually orthogonal domains so that in total four domains entered the calculations (with equal weights). Also, a mirror-symmetry plane was assumed to exist as (roughly) suggested by the STM image and as reasonable from the quasihexagonal arrangement of the oxide species on the quadratic substrate. It is indicated by the vertical line in Fig. 1(e) and limits the number of independent Co ions to five (denoted as Co1-Co5). The ion Co1 is assumed to reside in ideal bridge position while the others are in near-bridge or near-hollow positions or in between these cases (assuming the mirror plane to run through a Co ion in hollow position instead gave an R factor of 0.4 and thus was not further considered).

In order to improve the comparison of experimental and model spectra, the atomic positions were varied not only normal to the surface but also in-plane. Due to the mirror plane through ion Co1, this ion could only be varied in the two orthogonal directions within the mirror plane. The positions of the other four symmetrically inequivalent ions (Co2-Co5) were allowed to vary in all three dimensions. So, 14 structural parameters describe the geometry of this layer and the same applies to the number of parameters for the oxygen layer. Additionally, possible relaxations of the substrate atoms induced by the oxide had to be taken into account which were considered for the upper two iridium layers. As there are six symmetrically inequivalent atoms in the top substrate layer with two of them within the mirror plane the layer is described by 16 parameters. The positions of the five symmetrically inequivalent atoms in the second substrate layer can vary in all dimensions resulting in another 15 parameters so that the total surface is described by 59 structural parameters. Additionally, thermal vibrations of the various atoms and ions had to be considered. They were assumed to be isotropic whereby for the iridium atoms a vibration amplitude of 0.043 Å according to a bulk Debye temperature of 420 K was used. The amplitude of cobalt was allowed to vary as well as that of oxygen whereby, in the course of the structural analysis, different amplitudes were allowed for two different types of oxygen (for reasons described below).

A fit of this multitude of $N=62$ parameters is still justified by the huge database with a total-energy width of $\Delta E=18{,}000$ eV which, to our knowledge, is the largest database ever used for a LEED analysis. With the width of a single peak in a LEED spectrum amounting to $4V_{0i}$,[18] the database corresponds to $n=\Delta E/4V_{0i}=818$ independent data points. Thereby a redundancy factor of $n/N\approx13$ results so that a safe fit of all parameters can be assumed. Nevertheless, as a high-order multiparameter fit as in the present case might be influenced by unexpected parameter correlations the structural parameters derived should be carefully discussed with respect to their physical reasonability. This will be offered at the end of Sec. V.

We tested also nonstoichiometric models, i.e., models with a lower content of oxygen. On the basis of the average T-matrix approximation[22] implemented in the TENSERLEED program package[16] statistically distributed vacancies as well as even systematically missing ions could both be treated. Also models with locally differently stacked oxygen ions as suggested in Ref. 8 for a two-bilayer CoO film were checked. However, no indications for missing ions or deviations from regular CoO(111)-type stacking and 1:1 stoichiometry could be found in accordance with our spectroscopic results.

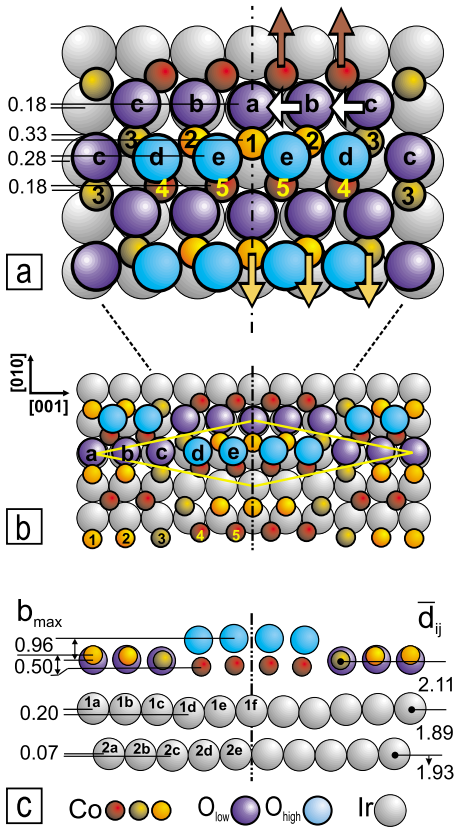

FIG. 2. (Color online) Top [(a) and (b)] and side (c) views of the best-fit structure with the applying mirror plane inserted as a vertical line and symmetrically inequivalent ions within the noncentered unit cell labeled. In the lower half of panel (b), only the cobalt species are displayed, the upper half contains also the oxygen. Co ions are small (red to yellow online) whereas O ions are larger (blue online). The numerical values of the maximum buckling amplitudes of layers $b_{\max}$ and the layers' spacings $\bar{d}_{ij}$ (with respect to the center of mass planes) are also displayed. All values are in angstrom units.

The fit procedure resulted in large deviations from the starting model (as described in detail below) and hence a good fit could only be reached after several iterations of the structural search with a new TENSORLEED reference calculation involved in each step. Not unusual for a multidimensional parameter search local minima in parameter space were found, one even with a R factor as low as 0.25. However, this could easily be identified as a nonglobal minimum through unphysical values of, e.g., the Co-O bond lengths. The final best-fit structure is displayed in Fig. 2 and the corresponding coordinates are summarized in Table I. The excellent quality of the best fit is mirrored by a R Factor of $R_{\min}=0.145$ with $R_i=0.102$ and $R_f=0.155$ applying to the subset of integer- and fractional-order beams, respectively. Of course, the visual comparison of experimental and best-fit data is also very favorable as demonstrated in Fig. 3 for a selection of beams.

The high quality of the fit also results in a high accuracy of the parameter values determined. The error limits can be estimated from the variance of the R factor,[18] $var(R)=R_{\min}\sqrt{8V_{0i}/\Delta E}=0.007$, whereby parameter sets leading to an R factor of $R>R_{\min}+var(R)=0.152$ can be excluded with high probability. Neglecting correlations between different parameters this leads to error margins for the z coordinates as low as ± 0.02 Å for the atom Co1 and ± 0.07 Å for the comparably weaker scatterer Oa which both are single atoms, i.e., not related to others by mirror symmetry, and so represent some kind of worst case.

TABLE I. Coordinates of the ions and atoms as labeled in Fig. 2(b). The coordinate z is vertical to and pointing into the surface with the value for the highest ion (Oe) taken as zero. The quantities x and y are the coordinates along [001] and [010] directions, respectively (as given in Figs. 1 and 2).

	x (Å)	y (Å)	z (Å)
Co1	0	−0.33	0.71
Co2	2.99	−0.32	0.75
Co3	5.96	−0.30	0.93
Co4	9.27	0.16	1.21
Co5	12.11	0.18	1.16
Oa	0	1.54	0.93
Ob	2.88	1.62	0.9
Oc	5.85	1.61	0.96
Od	9.03	1.62	0.07
Oe	12.06	1.64	0
Ir1a	0	1.36	3.00
Ir1b	2.75	1.33	3.03
Ir1c	5.49	1.37	3.05
Ir1d	8.18	1.35	3.20
Ir1e	10.85	1.36	3.13
Ir1f	13.57	1.35	3.10
Ir2a	1.36	0.03	4.94
Ir2b	4.06	0.02	4.98
Ir2c	6.79	0.01	5.01
Ir2d	9.49	−0.01	5.00
Ir2e	12.22	−0.01	4.96

The resulting best-fit model can be described as follows: the $c(10\times 2)$ superstructure is of 1:1 stoichiometry with nine Co and nine O species per ten Ir atoms. The oxide can be regarded as a heavily distorted CoO(111) bilayer. Rows of Co ions run between substrate Ir rows but locally the atomic positions deviate from the center line between those Ir rows in both directions with a total amplitude of 0.51 Å [Co1–Co5 in Fig. 2(a)]. Also, the lateral spacing between Co ions within one row varies by as much as 0.47 Å. The O ions relax laterally off the hollow positions formed by the Co ions toward the center of the underlying Ir rows from which they differ by a maximum of 0.28 Å (Oe) and a minimum of 0.18 Å (Oa) as also displayed in Fig. 2(a). Additionally, it can be seen that oxygen ions Ob and Oc are shifted toward the top positions of underlying Ir atoms.

Remarkably and unexpected, there are two different groups of O ions as displayed in a side view of the model [Fig. 2(c)]. Four of them (O_{high}) reside above the Co ions as assumed in the starting model of a nondisturbed CoO(111) bilayer. Yet, five O ions (O_{low}) are closer to the interface by

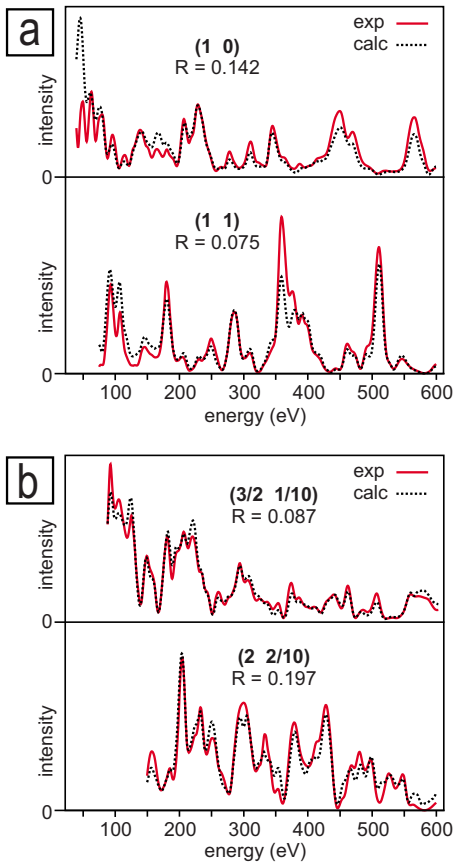

FIG. 3. (Color online) Comparison of experimental spectra (full line/red) and calculated model data (broken line/black) for (a) two integer-order beams and (b) two fractional-order beams. The single beam *R* factors are given in each case.

almost 1 Å and so are practically in-plane with their Co neighbors. This is why they were allowed to vibrate with different amplitudes in the course of the structure determination though, however, rather similar values resulted (0.12 Å for O_{high} and 0.14 Å for O_{low}; amplitude for Co: 0.10 Å). Laterally, the Co ions are placed further away from O_{low} ions and closer to O_{high} ions, leading to a wavelike in-plane distortion of the Co rows as indicated by arrows in Fig. 2(a). Normal to the surface the Co layer is buckled by 0.50 Å with an overall much larger distance from the Ir layer than expected from ionic Co hard-sphere radii. Last but not least the oxide film induces a considerable relaxation of the substrate. Ir atoms below the O_{low} ions relax outward leading to a buckling of the outermost Ir layer by 0.20 Å. The relaxation also propagates into the second Ir layer which is still buckled by 0.07 Å. Despite this rather strong induced corrugation of the outermost Ir layers, their center of mass distance is with 1.89 Å close to the value for a clean unreconstructed Ir surface of 1.85 Å.[23] The next average layer spacing (1.93 Å) is already bulklike justifying that oxide-induced relaxations had only to be considered for the first two substrate layers. The in-plane deviations from bulk positions are found to be rather moderate, namely, 0.06 Å(0.03 Å) for the first (second) Ir layer.

V. DISCUSSION

The height modulation of the oxide's protrusions imaged in STM [Fig. 1(d)] compares rather well with the crystallographic corrugation of the Co ions (but not with that of the O ions). Both, the corrugation pattern (three high, two intermediate, and four low-lying species) and the absolute corrugation amplitude (0.50 Å in geometry and 0.6 Å in STM) clearly prove that cobalt (and not oxygen) is imaged in STM. This had already been assumed before, however, based on rather uncertain grounds.[8] The present quantitative structure analysis also confirms the local positions of the Co ions postulated in our earlier work. Indeed, the Co ions are located between the Ir rows of the substrate with the position locally varying from bridge to hollow. The Co-Ir bond length between various pairs of Co and Ir varies only little (2.56–2.62 Å), i.e., a hard-sphere model with constant radii can be used as approximation. With $r_{Ir}=1.36$ Å, a value in the range 1.20–1.26 Å applies for Co with an average value of $r_{Co}=1.23$ Å. This is very close to the radius in metallic cobalt (1.26 Å) and far from the ionic radius in CoO (0.88 Å). Also, the Co-Ir bond length is rather close to that found for Co films grown on Ir(100)-(1×1), namely, 2.54 Å.[24] This means that the bonding of Co to Ir is dominantly of metallic/covalent character. This type of bonding might also be responsible for the fact that Co species are imaged in STM at very low bias voltages probing Co-related states at or close to the Fermi level.

While the positions of the Co ions result close to the model proposed earlier,[8] the location of part of the oxygen ions revealed in the present analysis comes as a surprise. Only four of the oxygen ions (O_{high}) are located, as expected, i.e., in or near hollow sites formed by the underlying Co ions. The Co-O_{high} bond lengths are with an average of 1.85 Å (variational range 1.81–1.87 Å) identical to that found for the outermost Co-O bonds in thicker CoO films,[4] where the local oxygen coordination is the same as in the present case. The other five oxygen ions (O_{low}), however, are pushed into the surface by almost 1 Å with respect to the other ones. As a consequence, they are practically coplanar with the surrounding Co ions and so cause the Co ions to shift sideward by some tenths of an angstrom [visualized by arrows in [010] direction in Fig. 2(a)] in order to maintain physically reasonable bond lengths. In fact, the Co-O_{low} bond length is with, on average, 1.94 Å (variational range 1.88–2.01 Å) even larger than that of Co-O_{high}, however, it is still much smaller than the value in the CoO bulk (2.13 Å). The low-lying oxygen ions are positioned close to the on-top sites of the Ir atoms below. Moreover, they also clearly relax laterally toward these on-top positions even at the expense of a significantly reduced distance between O_{low} ions (2.88 and 2.97 Å) as is visualized by arrows in [001] direction in Fig. 2(a) (note that the spacing of oxygen ions in the CoO bulk is 3.01 Å). As a consequence, the bonding distance of the O_{low} ions to the corresponding Ir atoms becomes extremely small (variational range 2.08–2.15 Å, average value 2.13 Å), the more so as these Ir atoms relax outward and even laterally just toward the coordinating oxygen ions. Using the elemental hard-sphere radius of Ir, a hard-sphere radius for O_{low} as small as 0.77 Å results. This

compares much more favorably to frequently observed values of 0.6–0.8 Å for covalent bonding of oxygen in adsorption systems (see, e.g., Ref. 25) than to the hard-sphere radius of O^{2-} [1.24–1.28 Å (Ref. 26)]. Similar small bond lengths of oxygen to the underlying substrate atoms had been found by quantitative LEED and density-functional theory (DFT) calculations for ultrathin vanadium oxide film on Pd(111) (Ref. 27) but unfortunately, they were not further discussed by the authors. Yet, it must be pointed out that such small bond lengths of oxygen ions appear not to be the rule. So, they are not observed even in other ultrathin cobalt-oxide films on Ir(100) as, e.g., in the recently investigated (3×3)-Co_5O_8 phase for which considerably larger values (2.72 Å and 2.83 Å) are reported.[7] The only common feature in both structures is that oxygen resides on-top of Ir or at least close to this site. In this respect, it differs from oxygen adsorbed on Ir(100) for which bridge site occupation is reported,[28] a site occupied by the nonbonding or less bonding O_{high} ions in the present case. Possibly, the different electronic and bonding properties of O_{low} ions are due to their simultaneous bonding to the Co species. Certainly, a deeper understanding of this phenomenon is highly desirable but may be only revealed by, e.g., future *ab initio* total-energy calculations.

With the bond lengths of cobalt and oxygen to substrate atoms being close to covalent bonds one might argue that the chemical scenario of our film may be better described as simple oxygen adsorption on a bimetallic Co-Ir substrate. Yet, for such a case, one should expect that the square symmetry which applies to Co/Ir(100) prior to the exposure to oxygen should be largely saved. As we have seen, this is not the case, i.e., the arrangement of Co and O species is quasihexagonal. As a consequence, the Co bonding to Ir loses its usual site specificity favoring a film-internal bonding and forming an oxide structure.

The local bonding of oxygen to Ir in on-top sites seems to play a crucial role for the understanding of the structure of the present CoO film. Obviously, it provides enough energy to squeeze the Co species apart, to contract the O_{low}-O_{low} distance, and to induce an outward movement of the coordinating Ir atoms. This interplay of competing forces prohibits almost any local symmetry both for the sites of oxygen and cobalt and even the bond lengths to nearest neighbors of the same type can result in rather different values. The large misfit between the lateral lattice parameters of bulk CoO and the Ir substrate (10%) prohibits the growth of a uniform and undisturbed (100) oriented film. Instead, the film grows in (111) orientation and is periodically distorted through local pinning induced by oxygen binding to Ir in or near on-top sites. So, a modulation of the oxide film by different structural elements results. Around the O_{high} ions the film assumes a rather regular rocksalt-type configuration. In contrast, the O_{low} ions form a local hexagonal boron-nitride-type (h-BN-type) structure as they are almost in-plane with Co ions. This is emphasized by the model representation given in Fig. 4 in which the two groups of oxygen are separated in two panels. Though recent first-principles calculations[29] reveal that CoO films (even when ultrathin) do not crystallize in h-BN structure, this phase seems to be at least energetically close to the wurtzite structure according to other DFT calculations for

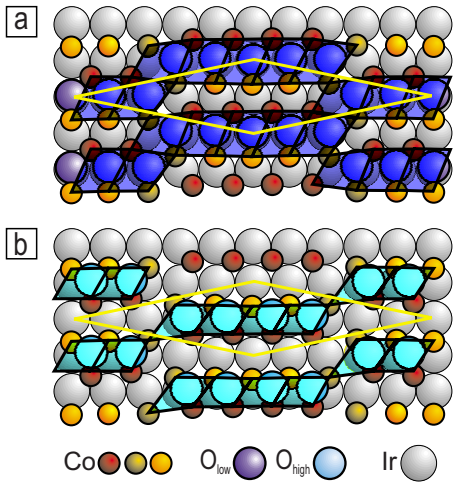

FIG. 4. (Color online) Separation of the two oxygen groups in two panels, namely, (a) with boron-nitride-type and (b) with rocksalt-type bonding. The distorted (quasihexagonal) unit cells are displayed in each case.

bulk CoO.[30] They find the wurtzite structure to be instable which leads to an in-plane arrangement of O and Co species. For that a hexagonal unit mesh length $a_W^*=3.476$ Å is calculated from which an in-plane Co-O bond length $L=a_W^*/\sqrt{3}=2.01$ Å results which fits to the range we find for Co-O_{low}. Since elements of the wurtzite structure have been found at the surface of CoO films,[3] which might be stabilized by the surface, and given the attractive interaction of O_{low} with the substrate the local appearance of a h-BN-type structure is not unlikely and there might be no energy cost with respect to the rocksalt configuration. So, a delicate energy balance between different local structures together with a considerable site dependence of the O-Ir bonding (in the presence of neighbored Co) appears to be responsible for the modulated structure which we have detected for the CoO bilayer film under investigation.

Eventually, we address the reliability of the structural model determined. It is well known that quantitative LEED can suffer from parameter correlations: The structural search can land in a rather favorable local (though not the absolute) minimum of the *R*-factor hyperspace by identifying wrong values for a subset of parameters whereby their negative influences on the *R*-factor level cancel each other largely (though not fully) and a seemingly convincing *R*-factor value results. As the elemental species are treated as point scatterers in the LEED calculation they can assume any unphysical mutual distance, in particular, they can come rather close to each other without any warning (except occasionally occurring divergences in the calculation). This is much different from a structural fit by DFT in which unphysical bond lengths combine with drastic energy costs. The only way in the case of quantitative LEED is a check of the physical reasonability and consistency of the model achieved. We discuss that for the low-lying oxygen species O_{low} as they present a special and surprising feature of the best-fit structure. Physically, the species O_{low} can only be low lying if and only if the coordinating Co species below shift to allow for reasonable Co-O_{low} bond lengths. Consistently this happens,

indeed, so that a h-BN-type configuration is produced. Even more, the shift applies only to these coordinating Co species and not to others and the range determined for the Co-O_{low} bond lengths is in agreement with independent DFT calculations. Also, only the Ir atoms below the O_{low} species are shifted outward (toward the latter) while the other Ir atoms remain within their plane. Again this is consistent with the above-discussed attractive Ir-O interaction.

Last but not least we mention that the reliability of the structure determination is also supported by the homogeneous pattern of the R factors of the 50 different single spot spectra. As many as 46 of them fall in the range $0<R<0.25$ (only one of them is 0.347 so exceeding 0.3), i.e., there are no beam spectra with a serious experiment-theory misfit which might be indicative for the structure found to be wrong.

VI. CONCLUSION

In conclusion, we found a CoO(111)-type bilayer on Ir(100)-(1×1) whose structure, by interaction with the substrate, is drastically distorted compared to that of the bulk-type bilayer. It forms a $c(10\times2)$ superstructure with nine Co and O species and ten Ir atoms per (noncentered) unit cell and the Co layer facing the substrate. This stoichiometry is supported both by XPS and TDS. As a surprise, five of the nine O ions locally form a h-BN-type structure with the oxygen ions being practically coplanar with the Co species. They also exhibit a rather short bond length to Ir atoms on whose top (or near top) they reside. This structure is in stark contrast to the termination of the CoO(111) rocksalt-type bulk structure. Qualitatively, this behavior can be explained by a strong local character of the binding to the Ir substrate pinning the oxide bilayer to the substrate in particular by the Ir-O bonding and thereby modulating the whole structure. Due to the extremely large database used (energy width $\Delta E=18,000$ eV), the superb comparison between experimental and calculated model LEED spectra as well as the consistency of the structural parameters retrieved the crystallographic structure found appears to be on safe grounds. Also, the resulting bond lengths compare well with those found in other oxide phases. The drastic modulation of the ultrathin oxide by local bonding to the substrate, which has been quantitatively revealed, shows that the substrate can be of extreme influence. This might be important for technical applications and also as a test case for first-principles calculations.

ACKNOWLEDGMENTS

The authors gratefully acknowledge financial support by Deutsche Forschungsgemeinschaft.

[1] V. Skumryev, S. Stoyanov, Y. Zhang, G. Hadjipanayis, D. Givord, and J. Nogués, Nature (London) **423**, 850 (2003).
[2] K. Biedermann, M. Gubo, L. Hammer, and K. Heinz, J. Phys.: Condens. Matter **21**, 185003 (2009).
[3] W. Meyer, D. Hock, K. Biedermann, M. Gubo, S. Müller, L. Hammer, and K. Heinz, Phys. Rev. Lett. **101**, 016103 (2008).
[4] W. Meyer, K. Biedermann, M. Gubo, L. Hammer, and K. Heinz, Phys. Rev. B **79**, 121403(R) (2009).
[5] S. I. Csiszar, M. W. Haverkort, Z. Hu, A. Tanaka, H. H. Hsieh, H. J. Lin, C. T. Chen, T. Hibma, and L. H. Tjeng, Phys. Rev. Lett. **95**, 187205 (2005).
[6] F. P. Netzer, Surf. Sci. **604**, 485 (2010).
[7] M. Gubo, C. Ebensperger, W. Meyer, L. Hammer, and K. Heinz, J. Phys.: Condens. Matter **21**, 474211 (2009).
[8] C. Giovanardi, L. Hammer, and K. Heinz, Phys. Rev. B **74**, 125429 (2006).
[9] J. Küppers and H. Michel, Appl. Surf. Sci. **3**, 179 (1979).
[10] K. Heinz, G. Schmidt, L. Hammer, and K. Müller, Phys. Rev. B **32**, 6214 (1985).
[11] D. Lerch, A. Klein, A. Schmidt, S. Müller, L. Hammer, K. Heinz, and M. Weinert, Phys. Rev. B **73**, 075430 (2006).
[12] I. Horcas, R. Fernandez, J. M. Gomez-Rodriguez, J. Colchero, J. Gomez-Herrero, and A. M. Baro, Rev. Sci. Instrum. **78**, 013705 (2007).
[13] K. Heinz, Rep. Prog. Phys. **58**, 637 (1995).
[14] P. J. Rous, J. B. Pendry, D. K. Saldin, K. Heinz, K. Müller, and N. Bickel, Phys. Rev. Lett. **57**, 2951 (1986).
[15] P. J. Rous and J. B. Pendry, Prog. Surf. Sci. **39**, 3 (1992).
[16] V. Blum and K. Heinz, Comput. Phys. Commun. **134**, 392 (2001).
[17] M. Kottcke and K. Heinz, Surf. Sci. **376**, 352 (1997).
[18] J. B. Pendry, J. Phys. C **13**, 937 (1980).
[19] J. Rundgren, Phys. Rev. B **68**, 125405 (2003).
[20] K. Heinz and L. Hammer, Prog. Surf. Sci. **84**, 2 (2009).
[21] J. Gustafson, A. Mikkelsen, M. Borg, J. N. Andersen, E. Lundgren, C. Klein, W. Hofer, M. Schmid, P. Varga, L. Köhler, G. Kresse, N. Kasper, A. Stierle, and H. Dosch, Phys. Rev. B **71**, 115442 (2005).
[22] R. Baudoing, Y. Gauthier, M. Lundberg, and J. Rundgren, J. Phys. C **19**, 2825 (1986).
[23] A. Schmidt, W. Meier, L. Hammer, and K. Heinz, J. Phys.: Condens. Matter **14**, 12353 (2002).
[24] W. Meyer, Ph.D. thesis, Universität Erlangen-Nürnberg, 2009.
[25] P. R. Watson, M. A. Van Hove, and K. Hermann, *NIST Surface Structure Data Base, Ver. 5.0* (National Institute of Standards and Technology, Gaithersburg, MD, 2004).
[26] http://www.webelements.com/oxygen/atomsizes.html
[27] C. Klein, G. Kresse, S. Surnev, F. P. Netzer, M. Schmid, and P. Varga, Phys. Rev. B **68**, 235416 (2003).
[28] K. Johnson, Q. Ge, S. Titmuss, and D. A. King, J. Chem. Phys. **112**, 10460 (2000).
[29] H. L. Meyerheim, C. Tusche, A. Ernst, S. Ostanin, I. V. Maznichenko, K. Mohseni, N. Jedrecy, J. Zegenhagen, J. Roy, I. Mertig, and J. Kirschner, Phys. Rev. Lett. **102**, 156102 (2009).
[30] T. Archer, R. Hanafin, and S. Sanvito, Phys. Rev. B **78**, 014431 (2008).